

## Carbon Allotropes

How to cite: *Angew. Chem. Int. Ed.* **2022**, *61*, e202205129

International Edition: doi.org/10.1002/anie.202205129

German Edition: doi.org/10.1002/ange.202205129

# The Microscopic Diamond Anvil Cell: Stabilization of Superhard, Superconducting Carbon Allotropes at Ambient Pressure

Xiaoyu Wang, Davide M. Proserpio, Corey Oses, Cormac Toher, Stefano Curtarolo, and Eva Zurek\*

**Abstract:** A metallic, covalently bonded carbon allotrope is predicted via first principles calculations. It is composed of an  $sp^3$  carbon framework that acts as a diamond anvil cell by constraining the distance between parallel *cis*-polyacetylene chains. The distance between these  $sp^2$  carbon atoms renders the phase metallic, and yields two well-nested nearly parallel bands that cross the Fermi level. Calculations show this phase is a conventional superconductor, with the motions of the  $sp^2$  carbons being key contributors to the electron–phonon coupling. The  $sp^3$  carbon atoms impart superior mechanical properties, with a predicted Vickers hardness of 48 GPa. This phase, metastable at ambient conditions, could be made by on-surface polymerization of graphene nanoribbons, followed by pressurization of the resulting 2D sheets. A family of multifunctional materials with tunable superconducting and mechanical properties could be derived from this phase by varying the  $sp^2$  versus  $sp^3$  carbon content, and by doping.

**M**etallic, covalently-bonded materials are candidates for conventional, or phonon-mediated, superconductivity.<sup>[1]</sup> Vibrations associated with the metallic covalent bonds, such as the B–B  $\sigma$  bonds in MgB<sub>2</sub>,<sup>[2]</sup> the C–C  $sp^3$  bonds in boron-

doped diamond,<sup>[3]</sup> and the weak multi-centered H–H bonds in the hydrogenic clathrate cages of compressed superhydrides<sup>[4]</sup> are characterized by a large electron–phonon coupling (EPC). The light mass of the constituent elements and the large density of states (DOS) at the Fermi level ( $E_F$ ) is key to achieving a high superconducting critical temperature,  $T_c$ . One way metallic covalent materials can be made is via the formation of unusual bonding environments induced by the high pressures present within diamond anvil cells. Carbon is particularly attractive since its strong bonds result in large kinetic barriers, important for quenching metastable materials to atmospheric pressures, and enhanced mechanical properties such as high density, superior hardness and large bulk modulus. Herein, density functional theory (DFT) calculations are performed to propose a form of carbon that is superconducting and superhard, and could be synthesized under mild pressures. Because it is characterized by an  $sp^3$  framework that behaves as a microscopic diamond anvil cell by constraining the distance between  $sp^2$  carbons, key for its metallicity, we call it DAC-carbon. Modifications of this structure could lead to a family of superconducting, superhard, multifunctional materials with tunable properties.

Previously, we predicted low-energy superhard carbon allotropes using a multi-objective evolutionary algorithm that employed both the DFT energy, and Vickers hardness ( $H_{v,Teter}$ ) estimated using shear moduli obtained via a machine learning (ML) model trained on the AFLOW database.<sup>[5]</sup> Forty-three novel superhard phases were found, and the topological properties of their carbon frameworks were analyzed. However, their electronic structures, bonding peculiarities, and propensity for superconductivity were not discussed.

Though most of the novel carbon allotropes were insulators with large gaps between the conduction and valence band, some were semiconductors, and two were metallic. DAC-carbon, referred to as *Cmmm*-12b in Ref [5] is one of these. Its primitive cell can be constructed by inserting  $sp^2$  carbon atoms in an all-*cis*-polyacetylene chain into the  $sp^3$  framework of the quasi-lonsdaleite structure R<sub>2</sub>L<sub>2</sub>,<sup>[6]</sup> commonly referred to as Z-carbon, and listed in the SACADA database<sup>[7]</sup> with the topology **sie** (Figure 1). At zero pressure DAC-carbon was 230 meV/atom (5.3 kcal mol<sup>-1</sup>) less stable than diamond (within the PBE functional), and its enthalpy fell below that of graphite above 40 GPa. Phonon calculations confirmed this phase was dynamically stable from 0–5 GPa at 0 K, and molecular dynamics (MD) simulations at 100, 200, 300 and 400 K on

[\*] X. Wang, Prof. E. Zurek

Department of Chemistry, State University of New York at Buffalo  
Buffalo, NY 14260-3000 (USA)  
E-mail: ezurek@buffalo.eduProf. D. M. Proserpio  
Dipartimento di Chimica, Universita' degli Studi di Milano  
Via Golgi 19, 20133 Milano (Italy)C. Oses, Prof. S. Curtarolo  
Department of Mechanical Engineering and Materials Science,  
Duke University  
Durham, NC 27708 (USA)C. Oses, Prof. C. Toher, Prof. S. Curtarolo  
Center for Autonomous Materials Design, Duke University  
Durham, NC 27708 (USA)Prof. C. Toher  
Department of Materials Science and Engineering, University of  
Texas at Dallas  
Richardson, TX 75080 (USA)  
and  
Department of Chemistry and Biochemistry, University of Texas at  
Dallas  
Richardson, TX 75080 (USA)

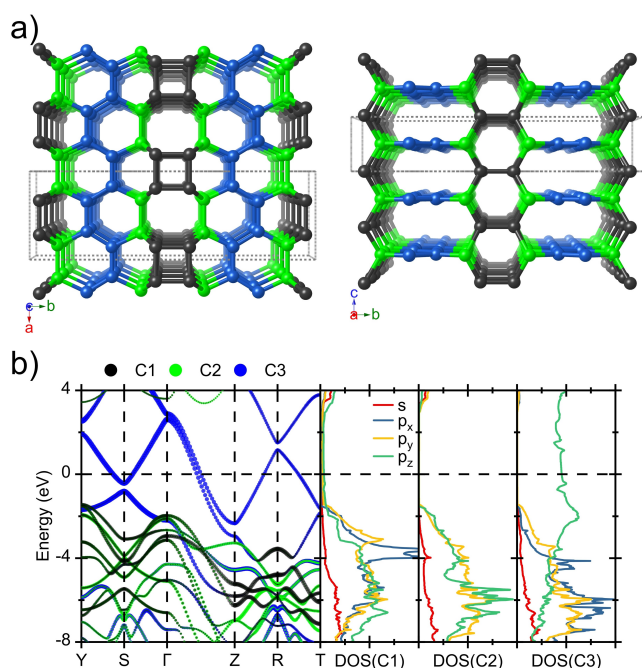


**Figure 1.** a) Optimized structure of DAC-carbon with top view and side view. Its standard primitive cell contains 12 carbon atoms (8  $sp^3$  and 4  $sp^2$ ) and possesses the  $Cmmm$  space group. Black balls are  $sp^3$  carbons that are bonded only to other  $sp^3$  carbons, green balls are  $sp^3$  carbons bonded to both  $sp^3$  and  $sp^2$  carbons, and blue balls are  $sp^2$  carbons; dashed lines denote the conventional cell. b) Band structure along the Y (0.5,0.5,0)  $\rightarrow$  S(0,0.5,0)  $\rightarrow$   $\Gamma$ (0,0,0)  $\rightarrow$  Z(0,0,0.5)  $\rightarrow$  R(0,0.5,0.5)  $\rightarrow$  T-(0.5,0.5,0.5) high symmetry lines, and orbital projected density of states (DOS, in states  $\text{eV}^{-1} \text{\AA}^{-3}$ ) for DAC-carbon. The thickness of the lines in the band structure denotes the contribution from the listed atom types.

the 20 and 40 GPa ground state geometries illustrated they were kinetically stable. Moreover, our MD simulations on the zero pressure geometry showed that the  $sp^2$  carbon atoms from adjacent polyacetylene layers only begin to interact at 1600 K, suggesting the kinetic barriers to decomposition are large. Using the ML (DFT) calculated shear modulus we found  $H_{v, \text{Teter}} = 45$  (48) GPa, as compared to 72 GPa for  $R_2L_2$ .<sup>[5]</sup> Insertion of the  $sp^2$  atoms into  $R_2L_2$  dramatically decreases its hardness, however thanks to its  $sp^3$  framework DAC-carbon still falls above the superhard threshold.

As described fully in the Supporting Information, a potential pathway for the realization of DAC-carbon would begin from 6-armchair graphene nanoribbons (6-AGNRs), which can nowadays be made with ease.<sup>[8]</sup> Analogous to the methods used to synthesize a biphenylene network with 4-, 6- and 8-membered rings,<sup>[9]</sup> on-surface polymerization of the 6-AGNRs could be used to make a 2D precursor network, which our PBE-D3 calculations compute to be  $\approx 110$  meV/atom more stable than the synthesized biphenylene network. This precursor to DAC-carbon is among one of many networks proposed by Li, He and co-workers in a high-throughput study of 2D carbon allotropes, where its properties were reported.<sup>[10]</sup> Finally, DAC-carbon could be synthesized by layering the precursor sheets on top of each other

followed by compression to  $\approx 20$  GPa. Thus, DAC-carbon could potentially be synthesized under pressure, similar to the carbon phases observed upon cold compression of graphite,<sup>[11]</sup> or made using shock compression.<sup>[12]</sup>

The  $sp^2$  chains in DAC-carbon propagate along the  $a$ -axis and are stacked along the  $c$ -axis. Their interlayer distance of 2.57  $\text{\AA}$ , dictated by the rigid framework of the  $sp^3$  carbons, is considerably smaller than within the *cis*-polyacetylene crystal, with measured inter-chain distances of 4.4  $\text{\AA}$ .<sup>[13]</sup> This geometrical feature of DAC-carbon is reminiscent of the infinite polyene chains imagined by Hoffmann et al., whose interchain distance of 2.50  $\text{\AA}$  induced the metallicity in this hypothetical  $sp^2$  carbon allotrope.<sup>[14]</sup> Hoffmann's work inspired the theoretical prediction of other 3D forms of carbon whose metallicity was induced by the steric confinement of the  $sp^2$  carbon atoms.<sup>[15]</sup> Many of the predicted phases possessed a high hardness due to their large  $sp^3$  ratio,<sup>[16–18]</sup> and the  $T_c$  of two that were not superhard was predicted to be 5 and 14 K,<sup>[19]</sup> but the mechanism of superconductivity was not analyzed.

The band structure and DOS plots of DAC-carbon (Figure 1b) clearly illustrated their metallicity stems from the  $p_z$  orbitals of the  $sp^2$  carbons. To explore this further we built a model where the  $sp^3$  carbons of DAC-carbon, whose bond lengths were nearly equal to those within diamond (1.57  $\text{\AA}$  vs. 1.55  $\text{\AA}$ ), were removed from the cell and the dangling bonds were saturated by hydrogens. The resulting layered *cis*-polyacetylene chain possessed a repeating  $C_4H_4$  unit where the C–C bonds measured 1.39 and 1.40  $\text{\AA}$  (c.f. 1.37  $\text{\AA}$  calculated for *cis*-polyacetylene), as in the relaxed DAC-carbon structure. Varying the interlayer distance, we computed the band gap and estimated the internal pressure caused by the confinement from the negative of the change in energy versus volume,  $P = -dE/dV$ , as obtained numerically via the central difference method. Figure 2a illustrates that within the PBE-D3 (HSE-06) functionals the band gap closed when the interlayer distance was 4.15 (3.85)  $\text{\AA}$  corresponding to a pressure of 0.19 (0.50) GPa. At the distance found in the optimized DAC-carbon lattice, the model system remained metallic and the internal pressure was calculated to be 15.9 GPa. Thus, the lattice of  $sp^3$  carbons comprising DAC-carbon can be thought of as a microscopic diamond anvil that exerts pressure on the *cis*-polyacetylene chain, thereby inducing metallicity.

To better understand the origin of the insulator-to-metal transition, the PBE band structure of the *cis*-polyacetylene chain (Figure 2b) was analyzed. When the interaction between neighboring layers is small the highest occupied (lowest unoccupied) crystal orbital at the Zone center corresponds to the  $1b_g$  ( $2a_u$ ) symmetry linear combination of  $p_z$  orbitals that are  $\pi$  bonding (antibonding) along the shorter, and  $\pi$  anti-bonding (bonding) along the longer C–C distance, as illustrated schematically in the inset. At the  $\Gamma$ -point they are  $p_z$   $\sigma$  anti-bonding with the next layer, whereas at the Z-point the  $p_z$   $\sigma$  interaction is favorable. This interaction, insignificant at large distances due to the negligible orbital overlap, becomes increasingly important as the interlayer distance decreases. When the distance is the same as in DAC-carbon, the bands are pushed high above

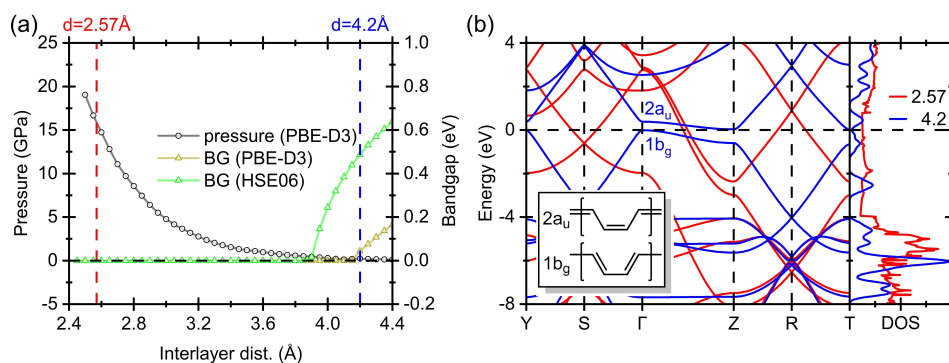


**Figure 2.** a) Band gap (BG) of an ensemble of *cis*-polyacetylene chains for the given interlayer distances as calculated with the non-hybrid PBE-D3 (brown triangles) and hybrid HSE-06 (green triangles) functionals. The pressure at these interlayer distances as obtained with PBE-D3 is also provided (black circles). b) Band structure as computed with the PBE functional for the *cis*-polyacetylene chain for interlayer distances of 4.20 Å (blue) and 2.57 Å (red). Since the interlayer spacing affects the *c* lattice constant, the length along the  $\Gamma$ -Z high-symmetry lines for the non-interacting chains has been scaled to match those whose distance is constrained to be the same as in DAC-carbon.

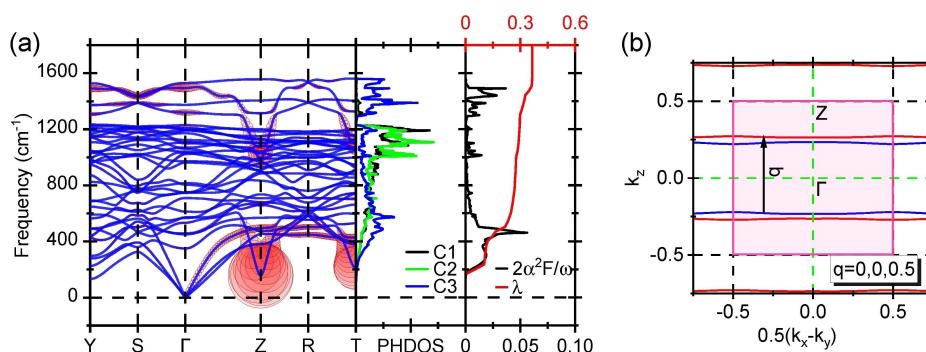


**Figure 3.** a) Phonon band structure, atom projected phonon density of states (PHDOS), Eliashberg spectral function, in the form of  $2\alpha^2F(\omega)/\omega$ , and the electron–phonon integral,  $\lambda(\omega)$ , for DAC-carbon. Red circles indicate the electron–phonon coupling constant,  $\lambda_{q\nu}$ , at mode  $\nu$  and wavevector  $\mathbf{q}$ , and their radii is proportional to the strength. b) Isocontour of eigenvalues for the two parallel bands  $1b_g$  (blue) and  $2a_u$  (red) at the Fermi level. The pink shaded region represents the first Brillouin zone. Black vector indicates the phonon vector  $\mathbf{q}=(0,0,0.5)$  by which the two bands are nested.

$E_F$  at the Zone center, and they run down to the Z-point nearly parallel to one another, as first proposed by Hoffmann for an all- $sp^2$  carbon analogue of the  $\text{ThSi}_2$  structure.<sup>[14]</sup> Near  $E_F$  the band structure we calculate for the squeezed *cis*-polyacetylene chain model is in strikingly good agreement with the bands obtained for DAC-carbon (cf. Figure 1b and Figure 2b). Though the  $p_z$   $\sigma$  bonding within DAC-carbon is weak (the integrated Crystal Orbital Hamilton Population for nearest neighbors is  $-0.06$  eV/bond, cf.  $-9.5$  eV/bond for the bonds in diamond), it is key for the metallicity of this phase.

This set of steep parallel bands separated by  $\approx 0.48$  eV suggests a Fermi surface that is well nested. Could DAC-carbon be a covalently bonded conventional superconductor? To answer this question, we calculated the phonon band structure, Eliashberg spectral function, the EPC parameter ( $\lambda=0.37$ ), and logarithmic average of the phonon frequencies ( $\omega_m=670$  K) for this phase. Within the Allen-Dynes modified McMillan equation, and using a renormalized Coulomb repulsion parameter characteristic of boron doped diamond,  $\mu=0.1$ ,  $T_c$  was estimated to be 1.6 K. This value is strikingly close to the only known superconducting

form of pure carbon, magic angle twisted bilayer graphene ( $T_c=1.7$  K), whose superconductivity is thought to be a result of strong electron correlations,<sup>[20]</sup> and somewhat lower than that of boron doped diamond ( $T_c=4$  K for a doping level of 2.5%).<sup>[21]</sup> The  $\lambda$  of DAC-carbon is similar to estimates for diamond doped with 1.85% boron,<sup>[22]</sup> even though its DOS at  $E_F$  is about a factor of five smaller.

To analyze the nature of the pairing mechanism, we plotted the phonon band structure decorated by the EPC line-widths, whose thickness is proportional to the coupling strength (Figure 3a). A soft mode with a frequency of  $156\text{ cm}^{-1}$  at the Z-point had the largest contribution, 26%, to the total  $\lambda$ . About 20% of  $\lambda$  was due to the four highest frequency bands, which are associated with the in-plane stretching modes of the  $sp^2$  carbons. These bands are relatively flat, but soften significantly around the Z-point. Careful inspection of the Fermi surface plots showed that the two parallel bands crossing  $E_F$  along the  $\Gamma\rightarrow Z$  line are strongly nested, so that an electron travelling on one of the surfaces can absorb a phonon with wavevector  $\mathbf{q}=(0,0,0.5)$  and be scattered on the other surface resulting in a large EPC (Figure 3b). Visualization of the vibration associated

with the  $156\text{ cm}^{-1}$  mode showed that it corresponded to the rotation of a pair of  $sp^2$  carbon atoms in the  $cb$  plane, with dimers in neighboring layers rotating in opposite directions, while the  $sp^3$  carbons remain stationary. This motion modified the distance between carbon atoms comprising neighboring polyacetylene chains, and the  $p_z$   $\sigma$  overlap between them.

Owing to the relatively heavy mass of carbon, the highest vibrational frequency in DAC-carbon is  $\approx 1600\text{ cm}^{-1}$ , and the  $\omega_{\text{in}}$  is relatively low. Because only the  $p_z$  orbitals of the  $sp^2$  carbons contribute to the metallicity, the DOS at  $E_{\text{F}}$  is also low. Both of these  $T_{\text{c}}$  descriptors could be increased via boron doping, and  $\omega_{\text{in}}$  could be improved by inserting  $\text{H}_2$  into the voids within the  $\text{R}_2\text{L}_2$  lattice. Since the weak  $p_z$   $\sigma$  interaction, which is dependent on the interlayer distance, is key for the EPC, the  $T_{\text{c}}$  is likely pressure dependent. Indeed, our calculations show  $T_{\text{c}}$  increases to 8.3 K at 5 GPa. The  $\text{R}_2\text{L}_2$  strips could be thickened thereby hardening the allotrope, but widening the  $sp^2$  chains would soften the material and increase the number of states participating in the EPC mechanism. Finally, different  $sp^3$  frameworks that comprise the microscopic diamond anvil can be chosen. We dream some of these multifunctional allotropes, where the carbon framework acts as a diamond anvil cell, will one day be experimentally realized.

### Acknowledgements

E.Z. and X.W. acknowledge the NSF (DMR-2119065), E.Z., C.T., C.O., and S.C. acknowledge the DOD-ONR (N00014-16-1-2583), and C.T., C.O., and S.C. acknowledge the DOD-ONR MURI program (N00014-15-1-2863) for financial support. The Center for Computational Research (CC) at SUNY Buffalo is acknowledged for computational support (<http://hdl.handle.net/10477/79221>).

### Conflict of Interest

The authors declare no conflict of interest.

### Data Availability Statement

The data that support the findings of this study are available in the Supporting Information of this article, and can be downloaded from the NOMAD repository and archive (10.17172/NOMAD/2022.06.17-1).

**Keywords:** Carbon Allotropes • Density Functional Calculations • Electronic Structure • Superconductors • Superhard Materials

- [1] X. Blase, E. Bustarret, C. Chapelier, T. Klein, C. Marcenat, *Nat. Mater.* **2009**, *8*, 375–382.
- [2] J. Kortus, I. I. Mazin, K. D. Belashchenko, V. P. Antropov, L. L. Boyer, *Phys. Rev. Lett.* **2001**, *86*, 4656.
- [3] L. Boeri, J. Kortus, O. K. Andersen, *Phys. Rev. Lett.* **2004**, *93*, 237002.
- [4] E. Zurek, T. Bi, *J. Chem. Phys.* **2019**, *150*, 050901.
- [5] P. Avery, X. Wang, C. Oses, E. Gossett, D. M. Proserpio, C. Toher, S. Curtarolo, E. Zurek, *npj Comput. Mater.* **2019**, *5*, 89.
- [6] R. Baughman, A. Liu, C. Cui, P. Schields, *Synth. Met.* **1997**, *86*, 2371–2374.
- [7] R. Hoffmann, A. A. Kabanov, A. A. Golov, D. M. Proserpio, *Angew. Chem. Int. Ed.* **2016**, *55*, 10962–10976; *Angew. Chem.* **2016**, *128*, 11122–11139.
- [8] N. Merino-Díez, J. Lobo-Checa, P. Nita, A. Garcia-Lekue, A. Basagni, G. Vasseur, F. Tiso, F. Sedona, P. K. Das, J. Fujii, I. Vobornik, M. Sambri, J. I. Pascual, J. E. Ortega, D. G. de Oteyza, *J. Phys. Chem. Lett.* **2018**, *9*, 2510–2517.
- [9] Q. Fan, L. Yan, M. W. Tripp, O. Krejčí, S. Dimosthenous, S. R. Kachel, M. Chen, A. S. Foster, U. Koert, P. Liljeroth, J. M. Gottfried, *Science* **2021**, *372*, 852–856.
- [10] X. Shi, S. Li, J. Li, T. Ouyang, C. Zhang, C. Tang, C. He, J. Zhong, *J. Phys. Chem. Lett.* **2021**, *12*, 11511–11519.
- [11] W. L. Mao, H.-k. Mao, P. J. Eng, T. P. Trainor, M. Newville, C.-c. Kao, D. L. Heinz, J. Shu, Y. Meng, R. J. Hemley, *Science* **2003**, *302*, 425–427.
- [12] C. He, C. Zhang, H. Xiao, L. Meng, J. Zhong, *Carbon* **2017**, *112*, 91–96.
- [13] R. Baughman, S. Hsu, G. Pez, A. Signorelli, *J. Chem. Phys.* **1978**, *68*, 5405–5409.
- [14] R. Hoffmann, T. Hughbanks, M. Kertesz, P. H. Bird, *J. Am. Chem. Soc.* **1983**, *105*, 4831–4832.
- [15] M. J. Bucknum, R. Hoffmann, *J. Am. Chem. Soc.* **1994**, *116*, 11456–11464.
- [16] X. Wu, X. Shi, M. Yao, S. Liu, X. Yang, L. Zhu, T. Cui, B. Liu, *Carbon* **2017**, *123*, 311–317.
- [17] L. Liu, M. Hu, Z. Zhao, Y. Pan, H. Dong, *Carbon* **2020**, *158*, 546–552.
- [18] Y. Liu, X. Jiang, J. Fu, J. Zhao, *Carbon* **2018**, *126*, 601–610.
- [19] M. Hu, X. Dong, B. Yang, B. Xu, D. Yu, J. He, *Phys. Chem. Chem. Phys.* **2015**, *17*, 13028–13033.
- [20] Y. Cao, V. Fatemi, S. Fang, K. Watanabe, T. Taniguchi, E. Kaxiras, P. Jarillo-Herrero, *Nature* **2018**, *556*, 43–50.
- [21] E. Ekimov, V. Sidorov, E. Bauer, N. Mel'nik, N. Curro, J. Thompson, S. Stishov, *Nature* **2004**, *428*, 542–545.
- [22] X. Blase, C. Adessi, D. Connétable, *Phys. Rev. Lett.* **2004**, *93*, 237004.

Manuscript received: April 7, 2022

Accepted manuscript online: June 8, 2022

Version of record online: June 24, 2022